Int. J. Electrochem. Sci., 11 **(2016)** 7216 – 7229, doi: 10.20964/2016.08.62

International Journal of ELECTROCHEMICAL SCIENCE
www.electrochemsci.org

Short Communication

Fabrication of Micro Annular Grooves on a Cylindrical Surface in Aluminum Alloys by Wire Electrochemical Micromachining

Wang Xiangyang[1], *Fang Xiaolong*[1,2], *Zeng Yongbin*[1,2,*], *Qu Ningsong*[1,2]

[1] College of Mechanical and Electrical Engineering, Nanjing University of Aeronautics and Astronautics, Nanjing, 210016, China
[2] Jiangsu Key Laboratory of Precision and Micro-Manufacturing Technology, Nanjing, 210016, China
[*]E-mail: binyz@nuaa.edu.cn

Received: 16 May 2016 / *Accepted:* 15 June 2016 / *Published:* 7 July 2016

Micro grooves, as a prominent microstructure in micro instruments, have been well applied in various industrial advanced applications. This study addressed to wire electrochemical micromachining (WECMM) of micro annular grooves on a cylindrical surface in an aluminum rod. By employing neutral electrolyte of sodium nitrate solution, the process would inevitably generate passive film on the surface at low current density. Thus, the dissolution characteristics of aluminum were experimentally analyzed by polarization curve. Under the optimized parameters, arrayed micro annular grooves with width of 100 μm, pitch of 80 μm and depth of 100 μm were fabricated on an aluminum rod with a diameter of 3 mm. This study revealed that WECMM is a promising method to produce micro annular grooves on a cylindrical surface in aluminum alloys.

Keywords: wire electrochemical micromachining, aluminum alloy, dissolution characteristic, micro annular grooves

1. INTRODUCTION

Miniaturization of micro instruments in aerospace, optical, microelectronics and biomedical has definitely been an emerging trend with numerous advantages, including low energy consumption rate, low cost, light weight and better product integration. Micro annular groove is a typical micro structure that has been widely used in micro instruments. For instance, in the fields of communication, micro grooves were introduced to design microwave sources of high performances with low return loss and the cross polarization level over a wide band [1]. In addition, micro grooves could be applied to reduce drag coefficient in some fluid mechanics cases as well [2-3].

Micro grooves could be fabricated by different processes, namely, turning, micro-grinding, electron discharge machining (EDM), laser machining and electrochemical machining (ECM). In some applications, micro grooves were generated on planar surface. Lee et al. [4] employed a LIGA process to fabricate micro-channels with width of 300 μm and depth of 200 μm on metallic bipolar plates. Schaller et al. [5] employed hard metal micro end mills to machine micro grooves with the achievement of minimum groove width of 50 μm for brass and 100 μm for stainless steel. By applying FIB-fabricated micro-tool, Adams et al. [6] successfully fabricated micro grooves with 13.2 μm in width and 4 μm in depth on cylindrical 6061-T6 aluminum rods.

Electrochemical machining (ECM) removes materials at atomic format with no contact between tool electrode and workpiece. Therefore, ECM could proceed with some inherent advantages namely no tool wear, no residual stress and damage-free surface without occurrence of heat-affected zone. Compared with the above-mentioned processes, ECM tends to be a promising method to fabricate micro grooves. Lee et al. [7] developed a prototype system in ECM to fabricate micro flow channels with 500 μm in width and 200 μm in depth on SS316 stainless steel. Natsu et al. [8] introduced a hybrid process that combined electrochemical jet machining and abrasive jet machining, and micro grooves with width of 235 μm and depth of 35 μm were produced. Liu et al. [9] employed pulse electrochemical sawing machining process to fabricate micro-inner annular groove that was 340 μm in depth and 263 μm in width on a 304 stainless steel tube.

Wire electrochemical micromachining (WECMM), which employs a metallic wire as the cathode, has the ability of fabricating plenty of complex microstructures such as through grooves [10], gears and helix coils. Zhu et al. [11] developed a micro wire electrochemical cutting process, and a series of complex micro structures with a slit width of 20 μm was fabricated on a 100 μm thick nickel plate. Shin et al. [12] reported to generate micro features such as micro through grooves and gears in stainless steel plates. By applying wire traveling and electrolyte flushing, Zeng et al. [13] successfully fabricated microstructures with feature heights up to 10 mm and feature aspect ratios of 50 or more by WECMM.

However, WECMM commonly provides an approach to produce micro grooves on planar surface, and the aspect ratio was less than 1. In this paper, investigations were focused on fabricating micro annular grooves on a cylindrical surface by WECMM. Besides, micro annular grooves were produced in aluminum alloys in this work. Aluminum alloys have been extensively used in technological and industrial applications due to their low density and high strength-to-weight ratio. In some applications, aluminum alloys need to be machined without recast layer nor heat-affected zone, and the structure dimension is on micron level. Thus inherent characteristics of WECMM enable itself to be a promising method to fabricate such micro grooves. A dense passive film will inevitably form on the surface during the machining process of aluminum by ECM [14]. Thus the dissolution characteristics of aluminum alloy in sodium nitrate solution were investigated. Moreover, the effect of machining parameters namely rotation speed, applied voltage, pulse frequency on machining stability and groove width were analyzed. Finally, arrayed micro annular grooves with aspect ratio of 1, in other words, width of 100 μm, pitch of 80 μm and depth of 100 μm were fabricated on an aluminum rod with a diameter of 3 mm.

2. METHOD AND EXPERIMENTAL APPARATUS

Fig.1 shows a schematic diagram of wire electrochemical micromachining to fabricate micro annular grooves on a cylindrical surface. The rotary aluminum rod attached to a spindle could move vertically (linear motion on z axis) during the process. The tungsten wire electrode acts as cathode and moves linearly along y axis, which is spatially perpendicular to the aluminum rod axis. During the machining process, a nozzle is employed to supply fresh electrolyte to the machining zone. In the machining process, the wire electrode is feeding towards the aluminum rod along linear trajectory with a constant feeding rate v_c. Gradually, a micro annular groove with the width of D is electrochemically machined with the rotation of the rod. To produce arrayed micro annular grooves, the wire electrode should be vertically drawn to a new position and repeat the above-mentioned process to fabricate another circular groove. Eventually, arrayed micro annular grooves with specific groove width and pitch on a cylindrical surface are fabricated after several repetitions.

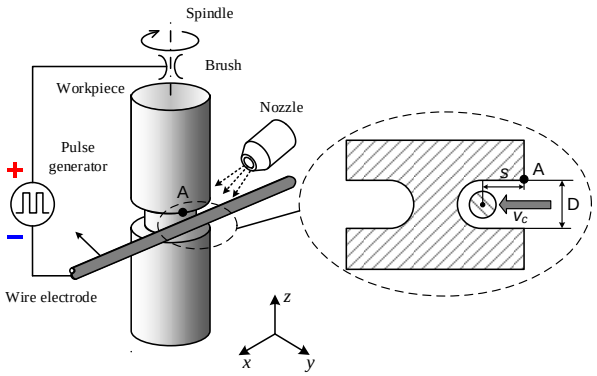

Figure 1. Schematic diagram of wire electrochemical micromachining.

The machining experiments have been performed on a self-developed WECMM system, as shown in Fig.2. The whole system consists of an X-Y-Z motion stage, a pulse generator, an oscilloscope, an electrolyte unit, fixtures and so on. The electrolyte unit contains an electrolyte pump and a nozzle is employed for the refreshment of electrolyte and removal of electrolytic product. A pulse generator supplies the electric voltage between the wire electrode and the workpiece which is rotating with the spindle. The entire machining process is observed by a charge coupled device (CCD), which is also beneficial for the initial tool setting.

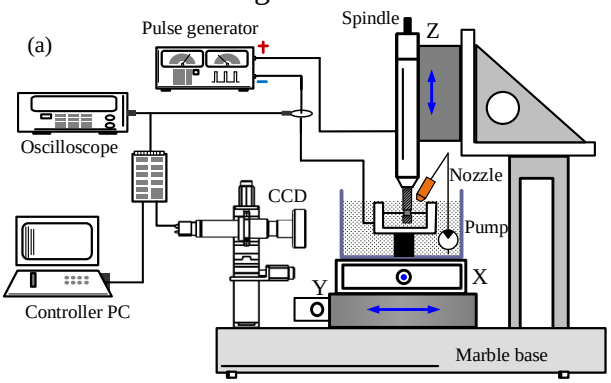

(b)

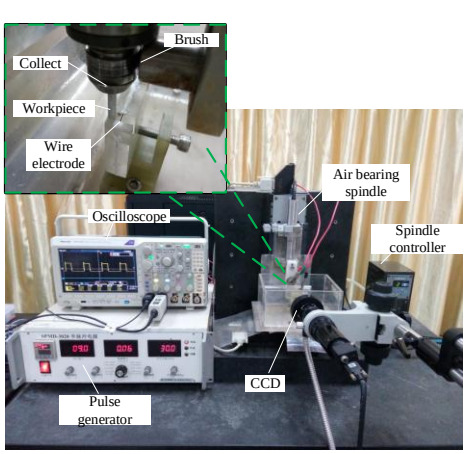

Figure 2. Experiment set-up for wire electrochemical micromachining. (a) Schematic of experimental apparatus, (b) Constructed experimental system.

Cylindrical specimens made of aluminum were 3 mm in diameter and 20 mm in length, which were cleaned ultrasonically before and after the experiments. The tungsten wire electrode was 20 μm in diameter. To determine the machining parameters and ensure the process stability, pre-trials were carried out as the reference. From the suggestions of pre-trials, the experimental conditions chosen are listed in Table 1. Moreover, to investigate a single experimental condition's effect to the machining process, the single factor experiments of the condition was conducted on the same aluminum rod. A scanning electron microscope (S-3400N, Hitachi, Japan) was used to measure the machined micro grooves.

Table 1. Experimental conditions.

Parameters	*Value*
Electrolyte	*15 g/L $NaNO_3$*
Applied voltage(V)	*8.5,9,9.5,10*
Pulse frequency(kHz)	*50,100,150,200*
Duty ratio(%)	*30*
Rotation speed(rpm)	*500,1000,2000,3000*
Electrode feed rate(μm/s)	*0.2*

3. RESULTS AND DISCUSSION

3.1. Dissolution characteristics of aluminum

In electrochemical machining of aluminum, the formation of a dense passive film is inevitable, which may inhibit the continuous dissolution process [15]. The pre-trials showed that at low current density, the machining accuracy and stability were poor. To investigate the influence of the passive film in electrochemical machining process, the dissolution characteristics of aluminum in 15g/L sodium nitrate solution were analyzed. Performed in a CHI66D electrochemical workstation, the

measurement of anodic polarization curve was carried out by using a platinum net and a calomel electrode as the counter-electrode and reference electrode respectively. The scanning rate in the tests was 1 mV/s, starting from -1 V to 5 V. It can be seen from the polarization curve presented in Fig.3 that between 0.2 V and 1.9 V only a slight increase of current density is detected, which indicates a passive region obviously. Barely no anodic dissolution takes place in the passive region. When the anode potential keeps increasing from 1.9 V, the current density enters into transpassive region, a steep increase of current density occurs due to the break of passive film. Thus the anodic dissolution takes the lead.

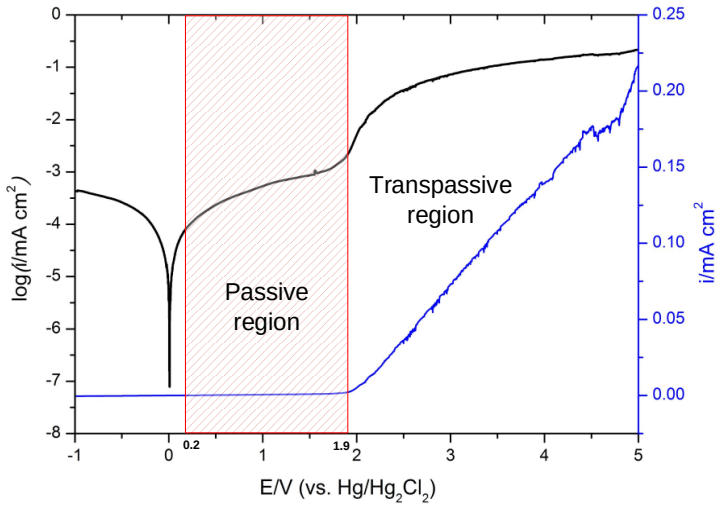

Figure 3. Polarization curve of aluminum in sodium nitrate solution.

The formation of the passive film can be illustrated in Fig.4. First of all, the initial air-formed film would easily break after applying voltage. Anodic and cathodic processes of aluminum electrochemical machining in sodium nitrate solution are respectively dissolution of aluminum and reduction of dissolved oxygen, as the following reactions show:

$$4Al \rightarrow 4Al^{3+} + 12e^- \quad (1)$$

$$3O_2 + 6H_2O + 12e^- \rightarrow 12OH^- \quad (2)$$

Then, Al^{3+} reacts with OH^- chemically to form aluminum hydroxide on the surface according to the following reaction:

$$4Al + 3O_2 + 6H_2O \rightarrow 4Al(OH)_3 \quad (3)$$

At last, due to it's low solubility, this hydroxide precipitates on the surface before it changes to aluminum oxide gradually, forming the passive film:

$$2Al(OH)_3 \rightarrow (Al_2O_3) + 3H_2O \quad (4)$$

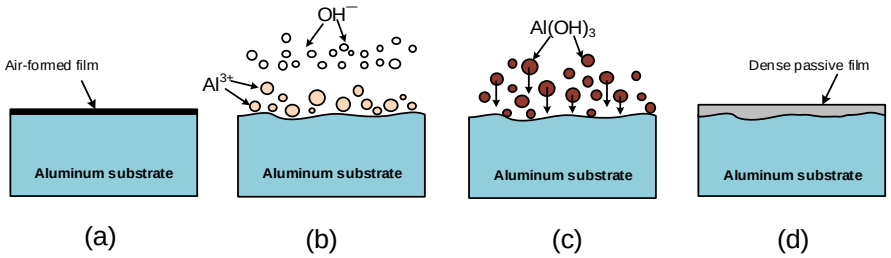

Figure 4. Schematic diagram of the electrochemical dissolution behavior of aluminum at low current density in sodium nitrate solution.

When it is exposed to corrosion solution, the passive film will soon break in the presence of aggressive anions [16]. Micro grooves machined by electrolyte of dilute hydrochloric acid in aluminum rod were presented in Fig.5, serious stray corrosion occurred on the surface. It could be reasoned that with no passive film formed in zones which were not expected to be machined, material dissolution also took place there, which resulted in stray corrosion. However, in sodium nitrate solution, which is neutral, the passive film only breaks with the increase of current density. A same phenomenon was also reported by Wang et al. [17]. Therefore, the passive film formed in non-machining zone due to low current density there could prevent the surface from stray corrosion.

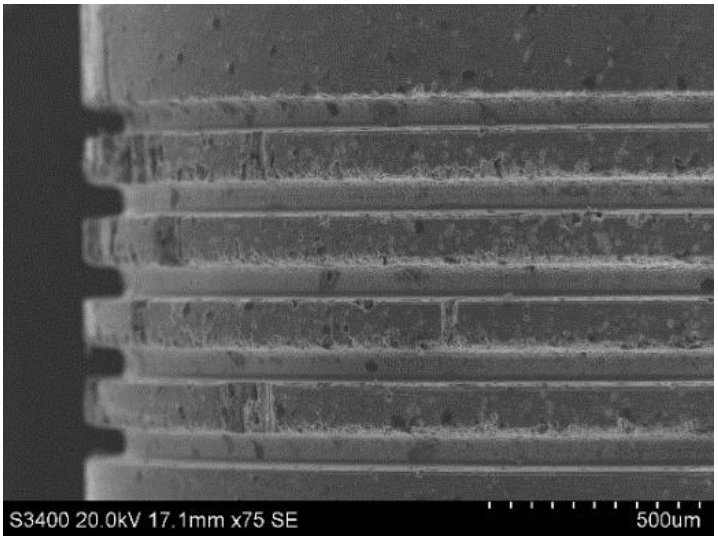

Figure 5. Micro grooves machined by dilute hydrochloric acid

The dissolution characteristics of aluminum have a great relation with the current density. Besides, unlike on a planar surface, the current distribution in processing micro groove on a cylindrical surface is a dynamic process. Therefore, to investigate the formation of the micro annular groove on an aluminum rod surface by WECMM, the analysis of the current distribution between the rod workpiece and wire electrode is significantly necessary.

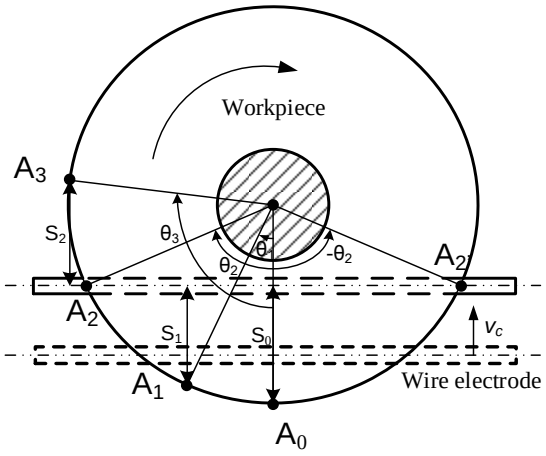

Figure 6. Top view of the fabrication process of micro annular groove.

A specific point where the cylindrical surface overlaps with the machined side gap, which is named as *A*, is typically marked to form a vertical distance *S* with the center line of wire electrode, as shown in Fig.6. The current density between the point *A* and wire electrode changes with the rotation of the workpiece, in other words, the phase angle of point *A* to circle center. From the top view of the machining process as shown in Fig.6, it is obvious that when the phase angel is 0°, there is a certain vertical distance S_0 between the workpiece and wire electrode. As a result, the current density doesn't reach the peak there. When the phase angle comes to θ_1, with the decrease of the distance, the current density increases. The two phase angle θ_2 and $-\theta_2$, where point A overlaps with wire electrode from the top view, share the highest current density. While the phase angle passes through the overlap point, the current density decreases again because of the increase of the distance. Moreover, with the wire electrode feeding towards the center of workpiece, the phase angle where current density reaches the peak becomes bigger.

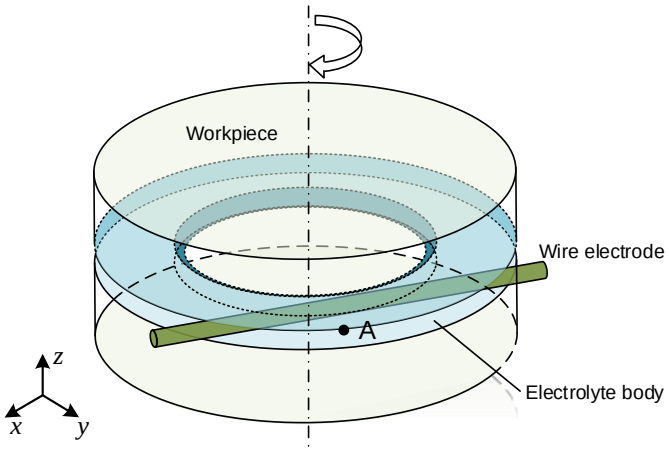

Figure 7. Electrolyte body in the inter-electrode gap of WECMM.

Table 2. Parameters applied in electric field simulation.

Parameters	*Value*
Workpiece diameter(mm)	*3*
Wire electrode diameter(μm)	*20*
Spindle speed(rpm)	*2000*
Groove width(μm)	*100*
Machined length(μm)	*25,50,75,100*
Electrolyte electrical conductivity(S/m)	*2*
Applied voltage(V)	*9*

A three-dimensional electrical model is set up as presented in Fig.7. The simulation was performed via COMSOL version 5.0. The parameters used in the simulation are listed in Table 2. Variations of the current density with phase angle are shown in Fig.8. Current density increases first, after the overlap phase angle, it decreases again. The current density curves of different feeding depths are also presented in Fig.8. As the wire electrode is feeding towards the workpiece, the current density decreases in general due to the increase of distance *S*. And because of the phase angle where point *A* overlaps with wire electrode becomes bigger, the peak current density angle increases accordingly. When the feeding depth is 25 μm, the peak current density is 160 A/cm^2 and the peak phase angle is 13 ° . As the feeding depth comes to 100 μm, the peak current density is 100 A/cm^2 and the peak phase angle is 30° . This indicates that with the feeding of wire electrode, the area which is relatively far from the wire electrode, can be defined as non-machining area as the current density there is low. So barely no aluminum dissolution takes places there. Thus, while the wire electrode feeds along the linear trajectory, the groove width homogeneity behind it can be ensured.

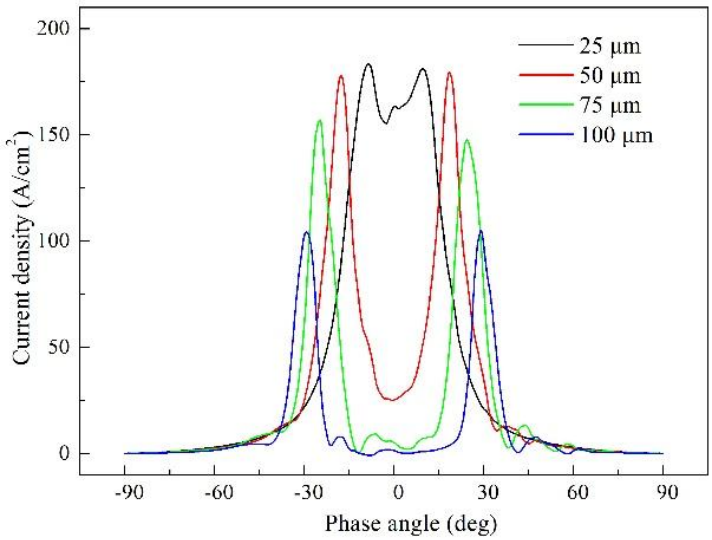

Figure 8. Variations of the current density with phase angle.

3.2 Effect of rotation speed

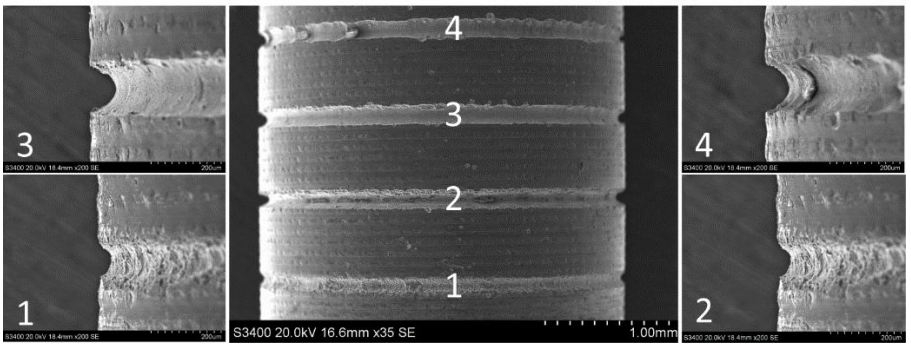

Figure 9. Effect of rotation speed on the micro groove width (1: 500rpm, 2: 1000rpm, 3: 2000rpm, 4: 3000rpm).

The effect of rotation speed on groove width was studied by the following fixed machining parameters: applied voltage of 9 V, pulse frequency of 200 kHz. Fig.9 shows the micro grooves machined by different rotation speed of the aluminum rod. The rotation speeds used in experiments were 500 rpm, 1000 rpm, 2000 rpm and 3000 rpm respectively, among which 2000 rpm was proved to fabricate the groove with widest width and best machining stability and surface quality. The groove width decreased dramatically when the rotation speed was higher and lower than 2000 rpm, but electrical short circuits occurred frequently meanwhile.

As shown in Fig.10, the transfer mechanism of the electrolytic products and electrolyte in machining area are illustrated by different levels of rotation speed. While the workpiece rotates with the spindle during machining process, electrolyte and electrolytic products moves with it by the viscosity of fluids. When the rotation speed is low, in the experiment circumstance were 500 rpm and 1000 rpm, the motion of electrolyte and electrolytic products around the workpiece are slow as well. Electrolyte in the machining zone is consumed quickly without timely supply. Meanwhile, the electrolytic products crow in the machining area as the removal of them is slow. As a result, the electrical conductivity is at a low level. Hence, the current density in machining area is low accordingly, which is not beneficial for the continuous material dissolution because of the formation of passive film, decreasing the machining efficiency and stability [14-15]. That explains the frequent occurrence of electrical short circuits and poor surface quality.

A different situation appears when the rotation speed is at medium level, in other words, appropriate level. As the workpiece rotation speed becomes higher, the flow speed around it increases therewith. Therefore the supply of the electrolyte is timely with the flow, and the removal of the electrolyte products is also guaranteed, ensuring that the electrical conductivity is stable for machining process. Thus the current density is high enough to pass into the transpassive region, where passive film is not formed and the aluminum rod dissolution is the priority.

However, as the rotation speed of the aluminum rod keeps increasing to a certain extent, the material removal and machining stability decreased in the experiments. As shown in Fig.9(c), the electrolyte is pushed away radially from the workpiece due to high centrifugal force. And because the

machining area was in open environment, not immerging in the electrolyte, an electrolyte evacuation gap appears consequently. Therefore, the current density turns back to the passive region where the passive film would be formed, inhibiting the dissolution process. As a result, the machining stability is poor when the rotation speed of the aluminum rod is too high.

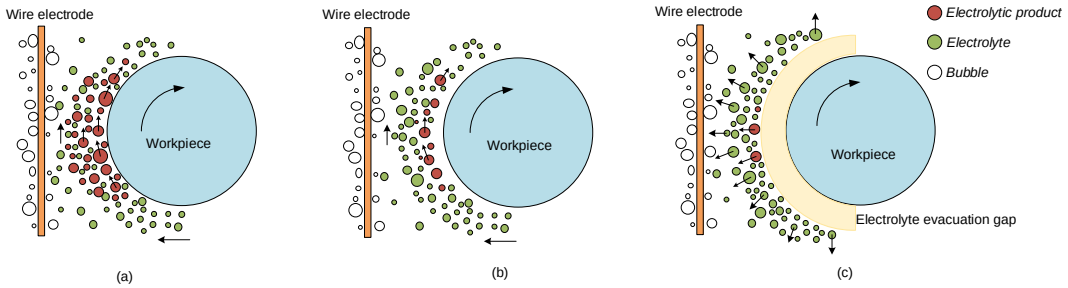

Figure 10. Transfer mechanism of the electrolytic products and electrolyte in machining area with different rotation speeds: (a) low speed; (b) medium speed; (c) high speed.

3.3. Effect of applied voltage

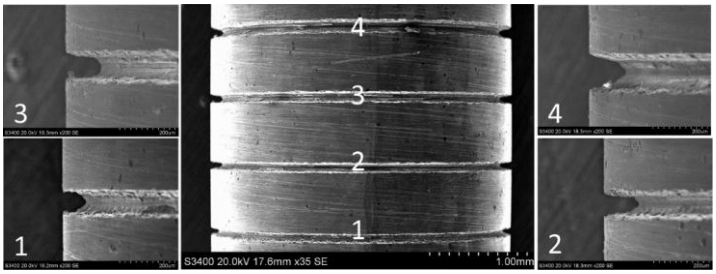

Figure 11. Effect of applied voltage on the micro groove width. (1: 8.5 V, 2: 9 V, 3: 9.5 V, 4: 10 V).

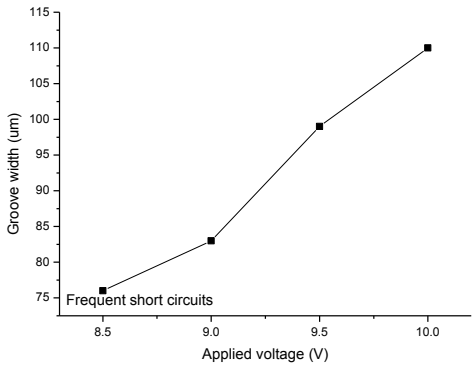

Figure 12. Variation of the groove width with applied voltage.

Fig.11 presents the micro grooves machined by different applied voltages between aluminum rod and wire electrode. And the variation of the groove width with applied voltage is presented in Fig.12. The fixed conditions are the rotation speed of 2000 rpm and pulse frequency of 150 kHz. The

groove width increased dramatically with the increase of applied voltage while electrical short circuits occurred frequently when it was 8.5 V. According to Faraday's law, the material removal rate, v_a, is determined by current density i as

$$v_a=\eta(i)\bullet\omega\bullet i \quad (5)$$

Where $\eta(i)$ is the current efficiency coefficient and ω is the material volumetric electrochemical equivalent. A high voltage results in a high current density [12, 18-19], thus the process enters into the transpassive region, where the material removal rate and the groove width were increased. When the applied voltage was 8.5 V, frequent electrical circuit shorts occurred. It could be reasoned that the current density in machining area is not high enough for continuous material dissolution because of the formation of passive film. However, as the applied voltage kept increasing from 9 V, the current density in non-machining area passed through passive region, causing un-wanted dissolution, stray corrosion would occur inevitably. Similar results were reported by B. Bhattacharyya et al. [20], they found stray corrosion and overcut when the applied voltage was large than 7 V. In this paper, 9 V was chosen as the most suitable applied voltage to fabricate micro grooves with good surface quality.

3.4. Effect of pulse frequency

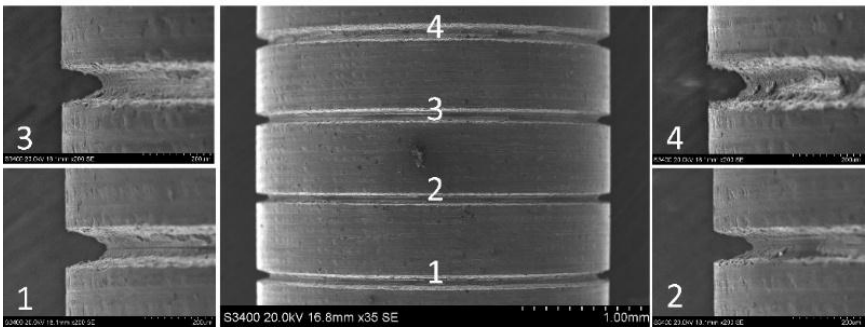

Figure 13. Effect of pulse frequency on the micro groove width (1: 50 kHz, 2: 100 kHz, 3: 150 kHz, 4: 200 kHz).

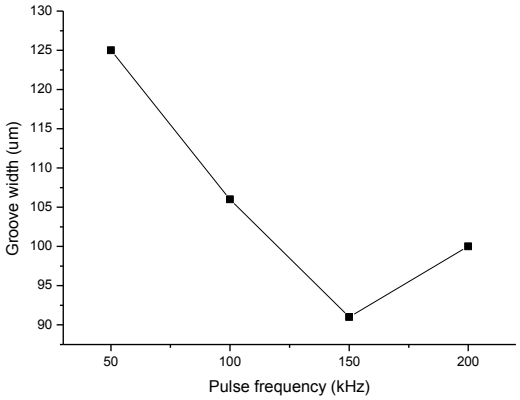

Figure 14. Variation of the groove width with pulse frequency.

With the fixed machining parameters: applied voltage of 9 V and rotation speed of 2000 rpm, the effect of pulse frequency on groove width was studied. Fig.13 presents the micro grooves machined by different pulse frequency. And the variation of the groove width with pulse frequency is presented in Fig.14. It can be seen from Figure.6 that 150 kHz took the position of fabricating the narrowest groove width among all the experimental pulse frequencies. When the pulse frequency increased from 50 kHz to 150 kHz, the groove width decreased accordingly. However, as the frequency value became bigger than 150 kHz, the groove width increased conversely. In addition, from the experimental results, no short circuits occurred when the pulse frequency was 150 kHz.

While the pulse voltage is introduced in fabricating aluminum by ECM, there are four processes in every pulse cycle, namely passive film formed, passive film broken, aluminum dissolution and electrolytic product removal. With the duty ratio fixed, pulse width becomes narrow with the increasing of pulse frequency, shortening the effective processing time. Thus the aluminum removal quantity decreases. It has been reported that high pulse frequency generates a shock wave, which is beneficial for the refreshment of electrolyte [21]. The renewal of electrolyte was strengthened from 150 kHz to 200 kHz consequently, resulting the current density in machining area increasing to high level for material removal. That explains the increase of groove width in 200 kHz. Therefore, 150 kHz was selected as a suitable pulse frequency fabricate micro grooves with narrow groove width and good machining stability.

3.5. Fabrication of arrayed micro annular grooves

With the investigation of the effect of different conditions on machining micro grooves on a cylindrical surface in aluminum alloys, an aluminum rod with arrayed micro annular grooves listed on the surface was fabricated with optimized experimental parameters, as shown in Fig.15. The machining conditions are sodium nitrate solution with a concentration of 15 g/L, a feed rate of 0.2 μm/s, applied voltage of 9 V, pulse duty of 30%, pulse frequency of 150 kHz and the rod rotation speed of 2000 rpm. The machined aluminum rod had good surface quality with no occurrence of stray corrosion, and had a groove width of 100 μm, pitch of 80 μm and depth of 100 μm, the aspect ratio was 1.

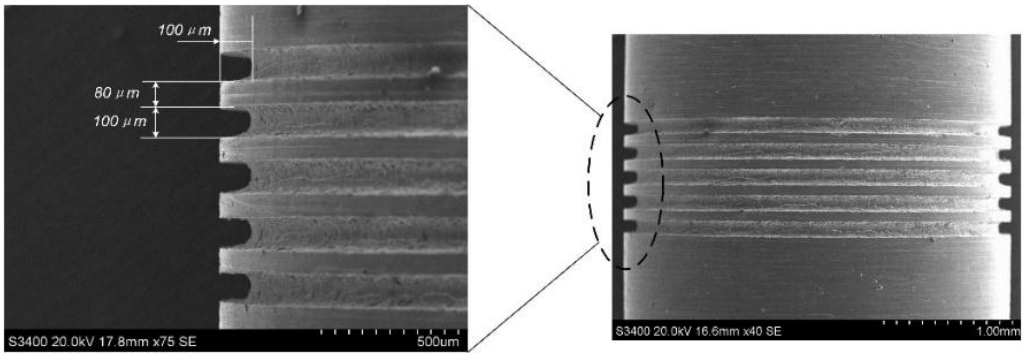

Figure 15. Arrayed micro annular grooves on the aluminum rod.

4. CONCLUSIONS

This paper has focused on the fabrication of micro annular grooves on a cylindrical surface in aluminum alloys by wire electrochemical micromachining (WECMM). Moreover, the polarization curve of aluminum in sodium nitrate solution was measured. Experimental investigations were carried out to study the influence of some key parameters on the groove width and machining stability, including workpiece rotation speed, applied voltage and pulse frequency. The conclusions can be summarized as follows:

(1) According to the polarization curve, a passive film will be formed at low current density. Barely no anodic dissolution takes place in the passive region. When the anode potential keeps increasing, a steep increase of current density will occur due to the break of the passive film. The fabrication of micro grooves in aluminum by WECMM should avoid the passive region for better material removal and machining stability.

(2) Optimized conditions, namely, applied voltage of 9 V, pulse frequency of 150 kHz and the rod rotation speed of 2000 rpm which were suitable for machining stability and accuracy, were employed to fabricate arrayed micro annular grooves with width of 100 μm, pitch of 80 μm and depth of 100 μm on an aluminum rod.

ACKNOWLEDGEMENTS
This project was supported by the National Natural Science Foundation of China (Grant no. 51375238), the China Postdoctoral Science Foundation funded project (Grant no. 2015T80546) and the Fundamental Research Funds for the Central Universities (Grant no. NZ2015207).

References

1. Y. Béniguel, A. Berthon, K. Van't, Klooster and L. Costes, *IEEE Transactions on Antennas and Propagation*, 53 (2005) 3540-3546
2. Yoichi Yamagishi and Makoto Oki, *Journal of Visualization*, 7 (2004) 209-216
3. Shinichi Takayama and Katsumi Aoki, *Journal of Visualization*, 8 (2005) 295-303
4. Shuo-Jen Lee, Yu-Pang Chen and Ching-Han Huang, *Journal of Power Sources*, 145 (2005) 369-375
5. Th Schaller, L Bohn, J Mayer and K Schubert, *Precision Engineering*, 23 (1999) 229-235
6. D.P Adams, M.J Vasile and A.S.M Krishnan, *Precision Engineering*, 24 (2000) 347-356
7. Shuo-Jen Lee, Chi-Yuan Lee, Kung-Ting Yang, Feng-Hui Kuan and Ping-Hung Lai, *Journal of Power Sources*, 185 (2008) 1115-1121
8. W. Natsu, S. Ooshiro and M. Kunieda, *CIRP Journal of Manufacturing Science and Technology*, 1 (2008) 27-34
9. Liu GX, Zhang YJ, Jiang SZ, Liu JW, Gyimah GK and Luo HP, *International Journal of Machine Tools and Manufacture*, 102 (2016) 22-34
10. Bo Hyun Kim, C.W. Na, Yun-Sil Lee and C.N. Chu, *CIRP Annals - Manufacturing Technology*, 54 (2005) 191-194
11. D. Zhu, K. Wang and N. S. Qu, *CIRP Annals - Manufacturing Technology*, 56 (2007) 241-244
12. Hong Shik Shin, Bo Hyun Kim and Chong Nam Chu, *Journal of Micromechanics and Microengineering*, 18 (2008) 1-6

13. Yong-Bin Zeng, Qia Yu, Shao-Hua Wang and D. Zhu, CIRP Annals - *Manufacturing Technology*, 61 (2012) 195-198
14. E. E. Coral-Escobar, M. A. Pech-Canul and M. I. Pech-Canul, *Journal of Solid State Electrochemistry*, 14 (2010) 803-810
15. S. Lameche-Djeghaba, A. Benchettara, A. Benchettara and V. Ji, *Arabian Journal for Science and Engineering*, 39 (2014) 113-122
16. A. Yurt, S. Ulutas and H. Dal, *Applied Surface Science*, 253 (2006) 919-925
17. Deng-Yong Wang, Zeng-Wei Zhu, Ning-Feng Wang, Di-Zhu and Hong-Rui Wang, *Electrochimica Acta*, 156 (2015) 30-307
18. Hai-Dong He, Yong-Bin Zeng and Ning-Song Qu, *Precision Engineering*, 45 (2016) 285-291
19. Malapati Manoj Kumar Reddy, *International Journal of Mechanical Engineering and Applications*, 4 (2013) 78-86
20. B. Bhattacharyya and J. Munda, *Journal of Materials Processing Technology*, 140 (2003) 287–291
21. Jung-Chou Hung, Chen-Hui Chang, Kuan-Chih Chiu and Shuo-Jen Lee, *International Journal of Advanced Manufacturing Technology*, 64 (2013) 813-820